

# Muscle Compliance and the Longitudinal Transmission of Mechanical Impulses

MARK SCHOENBERG, JAY B. WELLS, and  
RICHARD J. PODOLSKY

From the National Institute of Arthritis, Metabolism, and Digestive Diseases and the National Institute of Neurological Diseases and Stroke, National Institutes of Health, Bethesda, Maryland 20014

**ABSTRACT** The time required for a mechanical impulse to propagate from one end to the other was measured directly in frog sartorius muscles and in fiber bundles from the semitendinosus muscle. When the fibers were fully activated, the transmission velocity was 170 mm/ms. In resting fibers the transmission time was three to four times greater than in activated fibers. Control experiments indicated that the transmission time across the tendons was negligible. A muscle compliance of 55–80 Å per half sarcomere was estimated from these data. The “measurement time” of the method was calculated to be about 15  $\mu$ s. This relatively short measurement time makes the method potentially useful for detecting changes in cross-bridge compliance.

## INTRODUCTION

Evidence suggests that muscles are capable of generating force or shortening by means of attachments between the thin (actin) filaments and projections from the thick (myosin) filaments. A number of models have been advanced to describe the interaction. Virtually all of the models postulate that the cross bridges have two basic properties: the ability to detach from the actin filament at one site and reattach at another (cross-bridge turnover), and the capability of changing their length and/or angle of attachment during the period of attachment (conformational change). In some models the change in length or angle of attachment of the cross bridge occurs only when the thick and thin filaments move past each other (1, 2), while in a recent model (3) the conformational change is due to potential energy considerations and does not require any relative filament movement.

When the thick and thin filaments remain fixed relative to each other (as in isometric tension), it is practically impossible to distinguish between the various models. However, when the system is perturbed by either a change in length or load, the resultant changes in force or length depend upon the

kinetic properties of the cross bridges. It would be helpful, in distinguishing between various models, to be able to measure a property such as muscle stiffness at a given instant, in a manner uncomplicated by muscle cross-bridge turnover or time-dependent conformational change. In the present paper, a technique for measuring the transmission time of small longitudinal disturbances along muscle is described and its relation to "instantaneous" muscle stiffness is discussed. Since the technique can also be applied to shortening muscle, it may prove useful in answering many of the questions that have arisen (4, 5) concerning the rate constants of cross-bridge turnover.

#### *Past Work*

Experiments which measure muscle compliance have always been complicated by the presence of tendon compliance, apparatus compliance, and muscle shortening secondary to cross-bridge turnover. The first attempt to correct rigorously for some of these complications in direct measurements of muscle stiffness was made by A. V. Hill (6). Using the sartorius of *Rana temporaria*, he released a tetanized muscle to zero force at a rate of about 1.5 muscle lengths per second and measured the instantaneous force as a function of distance released. The muscle stiffness,  $K$ , was taken as the ratio of  $\Delta P$ , the change in force, to  $\Delta L$ , the displacement,

$$K = \frac{\Delta P}{\Delta L}. \quad (1)$$

The value of  $\Delta L$  was corrected for the apparatus compliance and "active" muscle shortening. The normalized, dimensionless value of the muscle stiffness,

$$\xi = \frac{\Delta P/P_o}{\Delta L/L}, \quad (2)$$

where  $P_o$  is the steady isometric force and  $L$  is the muscle length, came out to be 50. He repeated these experiments (7) releasing at a rate of four muscle lengths per second and the slope of the force-displacement curve at  $P_o$  corresponded to a normalized stiffness of 80.

Huxley and Simmons (3), using a high frequency response force transducer and a servosystem capable of producing release or stretch in just under a millisecond, measured the force just after a quick release or stretch. Using spot followers, thereby focusing on a central length of muscle, they were able to eliminate the effects of the tendon on compliance. The slope of their force-displacement curve at  $P_o$  for an isolated semitendinosus muscle fiber of *Rana temporaria* at 0–4°C showed a normalized stiffness of 130.

*Present Work*

The measurement of transmission time presented in this paper is essentially independent of cross-bridge turnover, time-dependent conformational change, and tendon connections. A whole sartorius muscle or small semitendinosus bundle, while generating full isometric tension, was quickly released at one end and the time for the disturbance in force to reach the other end was recorded using a high frequency force transducer. In the absence of internal viscosity, propagation time,  $\tau$ , down a long thin homogeneous elastic rod of length  $L$  and density  $\rho$  is

$$\tau = L(\rho/E)^{1/2}. \quad (3)$$

$E$  is Young's modulus of elasticity which is defined as

$$E = \frac{\Delta P/A^*}{\Delta L/L} \quad (4)$$

where  $A^*$  is the cross-sectional area that moves during small rapid displacements. If one calls  $\nu$  the fraction of the cross-sectional area of muscle that moves during small displacements, we have

$$A^* = A\nu, \quad (5)$$

where  $A$  is the cross-sectional area of the muscle.

From Eqs. 1, 2, and 4, we have

$$\xi = KL/P_o = EA^*/P_o. \quad (6)$$

From Eq. 3

$$E = \frac{L\rho}{\tau^2}. \quad (7)$$

Combining this with Eq. 6 gives the relation

$$\xi = \frac{ML\nu}{\tau^2 P_o}, \quad (8)$$

where  $M = AL\rho$ , the total mass. The only quantity which is not readily determined is  $\nu$ . This difficulty is discussed later.

Eq. 8 may appropriately be applied to determine the stiffness of a semitendinosus bundle where all of the muscle fibers are approximately the same length. In the whole sartorius muscle, where there is considerable dispersion of muscle fiber lengths, Eq. 8 must be modified. The experimental technique

used here measures the transmission time of the shortest fibers. Therefore  $L$ ,  $M$ , and  $P_o$  in Eq. 8 should all refer to the appropriate values for the shortest fibers,  $L_s$ ,  $M_s$ , and  $P_{os}$ . With the assumption that the shortest fibers produce the same force per unit area as the longer ones, we have

$$\frac{P_{os}L_s}{M_s} = \frac{P_oL_{AVE}}{M}, \quad (9)$$

where  $L_{AVE}$  is the average fiber length.

Substituting Eq. 9 into Eq. 8 yields

$$\xi_{\text{whole muscle}} = \frac{M_sL_s}{\tau^2P_{os}} \nu = \frac{ML}{\tau^2P_o} \nu \frac{(L_s/L)^2}{(L_{AVE}/L)}, \quad (10)$$

under the assumption that  $\nu_s = \nu$ .  $L$  in this case is any convenient reference length; for the sartorius, this is taken as the overall muscle length, which is equal to the length of the longest fibers. There is no reason to assume that the fraction of muscle mass accelerated in the shortest fibers of an entire muscle should be different from that of the muscle as a whole and the same is probably true for all but the smallest of muscle bundles. Single fibers (not used in the present study) might have a somewhat different value of  $\nu$  since the extracellular space between fibers is no longer present (see Discussion).

## METHODS

### *Mounting and Stimulation*

Sartorius muscles were dissected from the frog, *Rana pipiens*, leaving a small amount of bone at the pelvic end. The bone chip was then held by an aluminum clamp (270 mg) attached to a force transducer. The tendon was tied with a loop of 5-0 Deknatel silk as close to the muscle fibers as possible. The untied portion of tendon was looped tightly through a small ring which was rigidly attached to small diameter stainless steel tubing and this portion of tendon was tied over the original tie using a second loop of silk. A third loop was then tied around the first two ties, and the stainless steel tubing was attached to the displacement generator. For semitendinosus bundles, the tibial tendon was tied as described above while the smaller pelvic tendon was tied with a double square knot which was then secured with a third tie to the muscle clamp. The muscle, immersed within an acrylic plastic (Lucite) chamber, was bathed at a rate of approximately 2 vol/min with normal Ringer's solution composed of NaCl 115.5 mM, KCl 2.5 mM, CaCl<sub>2</sub> 1.8 mM, sodium phosphate buffer 3.1 mM, tubocurarine chloride 9 mg/l, at pH 7.0 at a temperature of 5.5–6°C. Striation spacing was adjusted to 2.2  $\mu\text{m}$  with the aid of a helium-neon laser. Overall muscle length was measured from the knot at the tendon end to the muscle-tendon junction at the pelvic end. The muscle was tetanized by passing current through platinum electrodes spaced 3 mm apart which spanned the entire length of the muscle and were used as alternate cathodes and anodes. The muscle was usually placed

about 1 mm from the stimulating electrodes and a voltage 1.5 times that giving a peak twitch response was passed using a Grass stimulator (Grass Instrument Co., Quincy, Mass.). At 6°C, pulses, 0.3–2.0 ms in duration at a frequency of 20–30 Hz, were passed for 300–500 ms.

### *Experimental Apparatus*

**DISPLACEMENT GENERATOR** A schematic diagram of the experimental setup is shown in Fig. 1. The displacement generator was built from a modified speaker coil assembly provided by Acoustics Research (Cambridge, Mass.). It had a maximum displacement of several millimeters and a natural frequency of 500 Hz. A 7-cm stain-

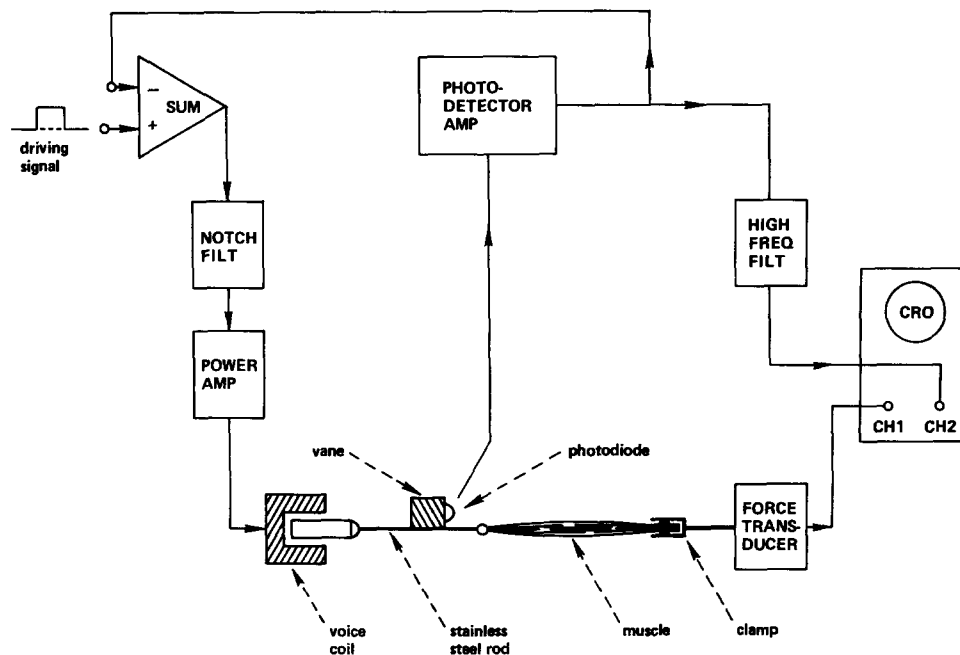


FIGURE 1. Schematic of experimental setup. SUM represents a group of high speed operational amplifiers, operated in the feedback mode, that compare the displacement signal from the displacement transducer (photodiode plus PHOTODETECTOR AMP) with the driving signal and produce an output signal proportional to the difference. This difference is fed through a notch filter (NOTCH FILT) to filter out the resonant frequency of the voice coil, and then fed into a power amplifier (POWER AMP) which drives the voice coil and produces a displacement proportional to the driving signal. A vane, attached through a stainless steel rod to the moving voice coil, decreases the amount of light (from a light-emitting diode not shown) falling on a photodiode, which is the first stage of the displacement transducer. The displacement transducer amplifiers have very high bandpass characteristics and the high frequency noise in the output signal is reduced using a filter (HIGH FREQ FILT) with a time constant of  $0.1 \mu\text{s}$  before the signal is fed into the oscilloscope (CRO) along with the signal from the FORCE TRANSDUCER.

less steel rod (diameter = 0.5 mm) was attached with epoxy cement to a Bakelite dome cemented to the voice coil. A small vane was attached to the rod for use with the displacement transducer described below.

The speaker coil could be operated in the feedback mode. In this mode, the signal from the displacement transducer was compared with a "driving signal," the difference amplified and fed into a Type 440K power operational amplifier (Opamp Labs, Los Angeles, Calif.) which drove the speaker coil. An asymmetric notch filter attenuated frequencies in the range of 500–1,000 Hz to help stabilize the feedback loop (necessary because of the resonant frequency of the assembly). It also amplified higher frequencies in order to compensate for the decreased frequency response of the coil above 500 Hz. Using high performance AD501 operational amplifiers (Analog Devices, Inc., Norwood, Mass.) the total lag in the feedback loop was under 10  $\mu$ s. Operation of the speaker coil in a feedback mode made it possible to achieve a linear relation between speaker position and driving signal. In this series of experiments, the feature was used only to keep the muscle at rest length during development of isometric tension. The displacement device operated in the feedback mode was not infinitely stiff. A force of 100 kdyn produced a displacement of 10  $\mu$ m. When the speaker coil was "maximally driven," the driving signal was large enough so that the power amplifier reached maximum voltage within 1–2  $\mu$ s and was unaffected by the feedback voltage from the displacement transducer. Under these conditions the speaker coil had a maximum velocity of 0.8 mm/ms and could accelerate to two-thirds maximal velocity in 0.1 ms.

**DISPLACEMENT TRANSDUCER** The displacement transducer consisted of a light-emitting diode (GE SSL-55B, General Electric Miniature Lamp Division, Schenectady, N. Y.), positioned 16 mm from a planar diffused silicon PIN photodiode (UDT-PIN-6DP, United Detector Technology Inc., Santa Monica, Calif.) with a slit,  $9 \times 1.6$  mm, positioned in front of the photodiode. Movement of the vane fixed to the speaker rod changed the intensity of light falling on the photodiode. One lead of the photodiode was grounded and the other connected directly to the negative input of an AD501 operational amplifier (Analog Devices) using a 50-k $\Omega$  feedback resistor. The positive lead of the operational amplifier was usually grounded although slightly increased sensitivity and frequency response could be obtained by biasing it by a few volts. Additional amplification ( $\times 2$ ) was obtained using a  $\mu$ A-741 operational amplifier. The rise time of the entire device in response to a pulse of light was less than 5  $\mu$ s. The transducer was linear to  $\pm 2\%$  over 0.75 mm of displacement and the sensitivity was 0.74 mV/ $\mu$ m. The ultrahigh frequency noise caused by the operational amplifiers was filtered at the output using a third order passive Butterworth filter with a time constant of 0.1  $\mu$ s. The largest amplitude of noise was from mechanical vibration. This was less than 2 mV or the equivalent of 3  $\mu$ m. The light-emitting diode was activated by supplying a constant current of 90 mA from a Kepco ABC-7.5 power supply (Kepco, Inc., Flushing, N. Y.). Long-term drift of the system was less than 4 mV.

**FORCE TRANSDUCER** The force transducer was a piezoelectric device (PCB 209A, PCB Piezotronics, Buffalo, New York). The natural frequency of the force

transducer was greater than 55 kHz. The relaxation time of the transducer was the order of 10 s. The sensitivity was 5.3 mV/kdyn. The noise was less than 0.5 mV and the long-term drift was less than 10 mV. In later experiments, a similar transducer, with a natural frequency of greater than 100 kHz, a relaxation time of 20 s, and a sensitivity of 5.0 mV/kdyn was used. The mechanical impulse at the end of the muscle was transmitted to the force transducer through a clamp, which introduced a fixed lag (the transmission time across the clamp) of about 6  $\mu$ s. The natural frequency of the force transducer with the clamp attached was less than 100 kHz, but this parameter is not important in transmission time measurements.

### *Technique*

During the plateau of isometric tension, the displacement generator was driven to cause as rapid a rate of shortening of the muscle as was possible with the present equipment. The force and displacement traces were simultaneously recorded on a dual beam Tektronix 5031 oscilloscope (Tektronix, Inc., Beaverton, Ore.). A steady voltage equal to the voltage output of the tension transducer at the time of release was subtracted from the force signal by using the differential inputs of the oscilloscope, in order that the sensitivity could be increased to 1–5 mV per division and the signal at the moment of release still appear on the oscilloscope face. The full voltage from the force transducer was also fed into a Tektronix R564B oscilloscope to record  $P_o$ . To avoid error due to relaxation of the tension transducer,  $P_o$  was taken as the total drop in force during the quick release, the release being rapid enough to drive the force to zero in a few tenths of a millisecond.

Typical records are shown in Fig. 2. Upward traces show displacement of the vane attached to the speaker coil (which, in the upper two records, drove the tendon end of the muscle in the direction of release). Downward traces show the force at the fixed end. The upper picture is from a 29.5-mm muscle and the middle picture from a 42-mm muscle. The artifact in the displacement trace, due to capacitative or inductive coupling between the transducer and the speaker coil, started at a fixed interval after a step in driving voltage to the displacement device. The time between the start of the voltage artifact (first arrow) to the earliest discernible decrease in force (second arrow) was measured. The transmission time along the muscle was taken as 50  $\mu$ s less than this time (see below). The lowest picture demonstrates the transmission time along a 12-cm low density polyethylene rod. The takeoff from base line of the force trace is much steeper because of the greater stiffness of polyethylene compared to that of muscle.

### *Accuracy and Calibration of the Technique*

There are two extraneous sources of delay in the measurement: fixed time lags in the apparatus and lags due to the finite response time of the force transducer and displacement generator. The latter can be minimized by increasing the recording sensitivity. Theoretical calculations based upon the response times of the various components suggested that the effects due to finite response time were small, and the calibration experiments described below substantiated this.

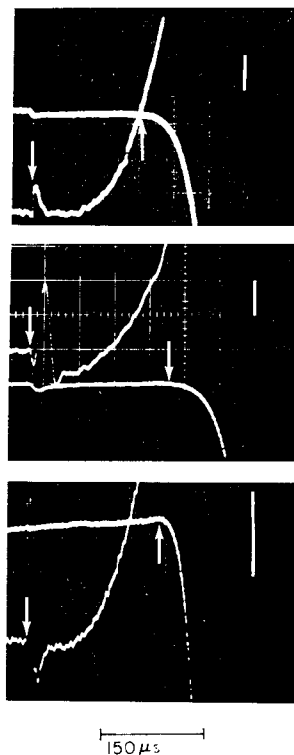


FIGURE 2. Typical records of force and displacement. Top record, 29.5-mm muscle ( $P_o = 48$  kdyn); middle record, 42-mm muscle ( $P_o = 92.5$  kdyn); bottom record, 12-cm low density polyethylene rod. Left arrow (on displacement trace) marks start of measured delay; right arrow (on force trace) marks end of measured delay. Transmission time along rod is  $34 \mu\text{s}$  less than measured delay (see Fig. 3). Transmission time along muscle is  $50 \mu\text{s}$  less than measured delay (see text). The vertical sensitivity markers denote 5 mV which corresponds to  $6.75 \mu\text{m}$  of displacement and 0.94 kdyn of force. The position of the arrow marking the end of delay was determined by placing a straightedge through the base line of the force trace and noting the earliest deviation of the trace from base line.

For calibration, rods of various lengths and different materials were mounted in the force transducer, the end of the 7-cm steel rod of the displacement generator was brought into contact with the test rod, and a very small but rapid displacement (representing compression or release) was applied. The time from the start of the displacement artifact to the change in force was measured.

As seen in Fig. 3, this time varied linearly with length as expected from Eq. 3 and intercepted the ordinate at approximately  $34 \mu\text{s}$ , due to fixed lags in the system. These fixed lags were due to the finite time necessary to get current into the coils of the speaker to accelerate the voice coil and also the finite time for the motion at the voice coil to be transmitted down the 7-cm steel rod attached to the coil. The latter was estimated to be approximately  $14 \mu\text{s}$  by positioning the vane and position transducer at two locations along the steel rod which were 5 cm apart and measuring a



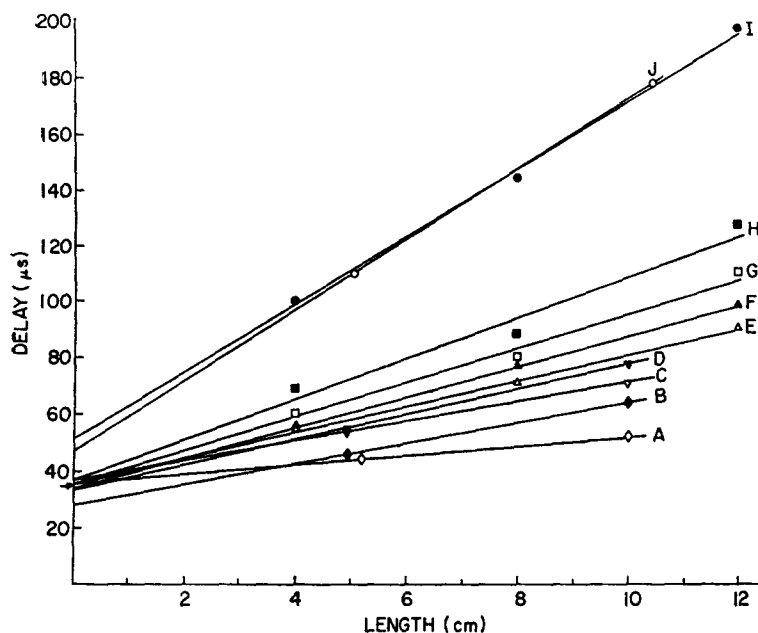


FIGURE 3. Measured delay times along different lengths of different types of rods. A, steel; B, brass; C, phenolic; D, Lucite; E, extruded polystyrene; F, cross-linked polystyrene; G, polypropylene; H, high density polyethylene; I, low density polyethylene; J, Teflon. Nearly all lines intersect the Y axis near  $34 \mu\text{s}$  (see arrow), the delay time with no rod in place. The records for lines I and J were difficult to read because the frequency components of the beginning of the fall in force due to release were similar to the frequency of standing waves present in the rod before release (caused by the interaction between vibration and the feedback loop). This problem did not exist in reading the records from muscle experiments (see Fig. 2) since there were no standing waves present in the resting or tetanized muscle.

time difference of  $10 \mu\text{s}$ . This agreed with the theoretical propagation speed for a steel rod. The intercept of  $34 \mu\text{s}$  was precisely the time recorded when the stainless steel rod was placed directly in contact with the force transducer. If, for each of the different types of rod material studied, the best straight line intercepting the ordinate at  $34 \mu\text{s}$  was drawn, most of the measured times deviated from this line by less than  $2 \mu\text{s}$ . The measured propagation speed down steel, aluminum, brass, and Lucite rods, for which reliable handbook values for density and stiffness were available, differed from the speeds calculated from Eq. 3 by less than 5%.

#### *Precision of the Measurement on Muscle*

In muscle experiments, a lag correction of  $50 \mu\text{s}$  was determined by allowing the muscle clamps to touch, generating a displacement, and measuring the time between artifact and change in force without a muscle in place. The extra  $16\text{-}\mu\text{s}$  correction was due to the additional length of steel and aluminum clamps. Repeat measurements of transmission time on a single muscle or measurements from the same record made by different observers rarely differed by more than  $10 \mu\text{s}$ .

## RESULTS

*Active Whole Muscle*

Fig. 4 shows the transmission times recorded from 18 tetanized muscles of different lengths released from  $P_o$  (the transmission time measured using stretch was identical to that measured with release). Data for the five longest muscles,  $L$  greater than 45 mm, were from *Rana pipiens berlandiari* from the Rio Grande valley rather than northern United States *Rana pipiens pipiens*, which were used in all the other experiments, and they were not included in the calculation of the least squares regression line which is shown in the figure. The least squares regression line is consistent with the assumption that transmission time is directly proportional to muscle length as suggested by Eq. 3, and that transmission speed is a characteristic property of muscle fibers. The average value of  $L/\tau$  for the 13 *Rana pipiens pipiens* sartorii was  $292 \pm 7$  mm/ms (mean  $\pm$  SEM). The average value of  $\rho P_o L/M$  was 1.9

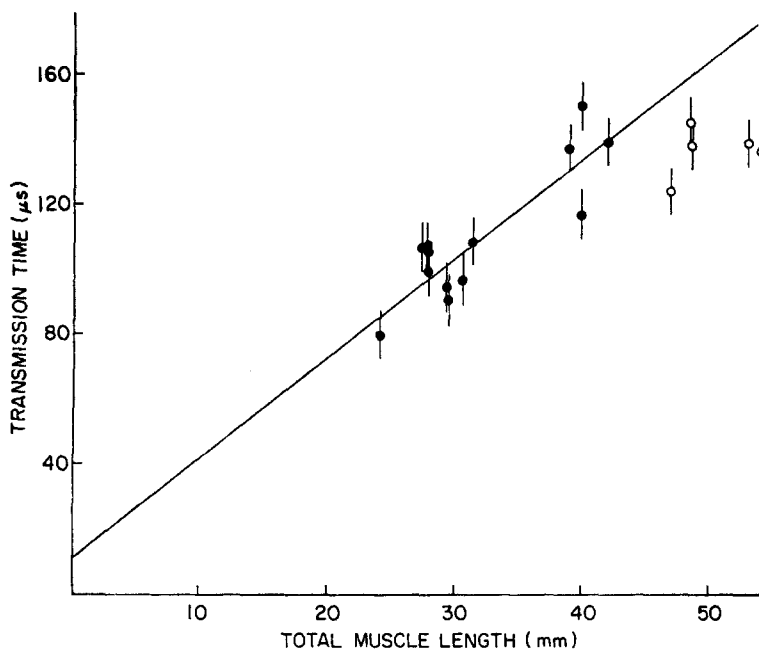


FIGURE 4. Transmission time measured at maximal force, in maximally tetanized frog sartorius muscles, as a function of total muscle length. Closed circles, *Rana pipiens pipiens*; open circles, *Rana pipiens berlandiari* (see text). Vertical lines represent estimated maximum uncertainty in measurement. The Y intercept of the least squares regression line for the *Rana pipiens pipiens* data points is  $11 \pm 17$ , not significantly different from zero. To obtain transmission time, total delay was corrected for apparatus delay ( $50 \mu\text{s}$ ), but not for extra delay due to tendon and tie ( $< 8 \mu\text{s}$ ).

TABLE I  
FULLY TETANIZED WHOLE SARTORIUS MUSCLES

Date	<i>L</i>	<i>M</i>	<i>P</i> <sub>0</sub>	$\rho P_0 L / M$	$\tau$	0.6 <i>L</i> / $\tau$	$\xi_{\nu=1}$ Eq. 10
	mm	mg	kdyn	Mdyn/cm <sup>2</sup>	$\mu$ s	mm/ms	
<i>Pipiens</i>							
12/4	39	210	63.7	1.24	138	170	291
12/7	40	152	79.6	2.1	151	159	150
2/14	42	182	92.5	2.13	140	180	190
1/8	29.6	73	65	2.62	95	187	167
1/17	30.7	76	51	2.02	97	190	222
1/22	28	83	46	1.55	107	157	199
1/23	28	67	47.6	1.96	106	158	160
1/24	29.5	66	48	2.17	91	194	218
1/29	31.4	90	50	1.74	109	173	215
2/5	24.2	43	27	1.52	80	182	272
2/7	27.5	37	23.7	1.77	107	154	168
2/13	39.8	148	67.5	1.82	117	204	286
5/1/A	28	40	37	2.59	100	168	136
mean				1.94		175	206
± SEM ( <i>N</i> = 13)				±.11		±4	±14
<i>Berlandiari</i>							
5/1/B	48.5	613	255	2.02	146	199	245
5/2	47	291	133	2.15	125	226	301
5/4	53	548	169	1.64	140	227	385
5/7	54	614	270	2.38	137	236	293
5/8	48.6	443	182	2.00	139	210	276
mean				2.04		220	300
± SEM ( <i>N</i> = 5)				±.12		±7	±23

*T* = 6°C; *L*, muscle length (also length of longest fibers); *M*, muscle mass; *P*<sub>0</sub>, steady tetanic force;  $\tau$ , transmission time along active muscle; 0.6 *L* /  $\tau$ , transmission speed along active muscle assuming length of shortest fibers, *L*<sub>s</sub>, is 0.6 *L* (see text);  $\xi_{\nu=1}$ , normalized stiffness ( $\nu = 1$ ) from Eq. 10 with *L*<sub>s</sub> = 0.6 *L*, *L*<sub>AVE</sub> = 0.8 *L*.

± 0.1 Mdyn/cm<sup>2</sup> ( $\rho$  for muscles was assumed equal to 1 g/cm<sup>3</sup>). The data are summarized in Table I.

#### *Resting Whole Muscle*

The transmission time along a 25–40-mm resting sartorius muscle was of the order of 300–400  $\mu$ s, about four times that in the activated muscle. Because of the small forces involved, the uncertainty of this measurement was the order of 100  $\mu$ s. No clear correlation between resting transmission time and muscle length was seen although because of the poor precision, this could not be ruled out. It is not known what elements in our preparations contributed to the resting propagation speed. The present results are in good

agreement with similar measurements made on resting sartorius muscle by Sandow (8).

### *Muscle Bundles*

Seven muscle bundles were dissected from the frog semitendinosus muscle. They contained 10–200 muscle fibers;  $P_o$  ranged from 0.54 to 14.6 kdyn. The average propagation speed along the tetanized muscle was  $169 \pm 11$  mm/ms. The results for each preparation appear in Table II.

### *Partially Activated Muscle*

Table III summarizes the results of a single transmission time experiment in which only some of the fibers of a whole muscle were activated. This was accomplished by applying submaximal stimulating voltages. This method was not ideal in that the time for the force to become relatively steady in-

TABLE II  
FULLY TETANIZED SEMITENDINOSUS MUSCLE BUNDLES

Date	$L$	$M$	$P_o$	$\rho P_o L/M$	$\tau$	$L/\tau$	$\xi_{\nu=1}$ Eq. 8
	mm	mg	kdyn	Mdyn/cm <sup>2</sup>	$\mu$ s	mm/ms	
6/20	15	1.4	0.5	0.54	115	130	240
6/26	16.4	6.8	6.3	1.5	77	213	302
6/28	14.0	3.0	2.5	1.1	82	171	265
7/11	16.6	6.0	2.6	0.72	88	189	496
7/13	13.9	7.6	14.6	2.7	79	176	115
7/19	14.1	2.0	2.0	1.4	84	168	201
7/20	10.0	4.5	3.4	0.76	74	135	240
mean				1.25		169	266
$\pm$ SEM ( $N = 7$ )				$\pm .3$		$\pm 11$	$\pm 44$

$T = 6^\circ\text{C}$ ;  $L$ , fiber length;  $M$ , muscle mass;  $P_o$ , tetanic force;  $\tau$ , transmission time along active muscle fiber bundle;  $\xi_{\nu=1}$ , normalized stiffness ( $\nu = 1$ ) from Eq. 8.

TABLE III  
RELATIVE TRANSMISSION TIME AND STIFFNESS  
IN A PARTIALLY ACTIVATED WHOLE MUSCLE

	Relative $P$	Relative $\tau$	Relative $\xi_{\nu=1}$
Control (start)	1	1	1
	0.49	1.09	1.72
	0.14	1.42	3.6
Control (finish)	0.87	1.02	1.10

Partial activation was achieved by stimulation with submaximal voltages at the same frequency as for the maximal tetanic response. Control values were  $\tau = 117 \mu\text{s}$ ,  $\rho P_o L/M = 1.82$  Mdyn/cm<sup>2</sup>. ( $L = 39.8$  mm).

creased from 300 to 700 ms for subthreshold stimulation, and probably some of the fibers were only partially tetanized. A detailed discussion of the results is given in the Discussion.

#### *Muscles in Rigor*

Four muscles, 28–31 mm long, were put in rigor by adding 0.5 mM iodoacetic acid to normal Ringer's solution at room temperature and stimulating the muscle once every 2 s until the force generated at each shock was less than 0.4 kdyn. Resting tension and transmission time in this state were quite variable from muscle to muscle. However, one consistent finding was that if iodoacetate-poisoned muscles were stretched by 1 mm the transmission time decreased by approximately 10  $\mu$ s whereas if they were relaxed by 1 mm, the transmission time was unmeasurable, i.e. there was no measurable change in force in response to a quick release. The transmission time of active muscle was independent of changes in length of the order of 1 mm.

#### *Tendon Control*

In order to assess any delays due to the tendons and the tie to the displacement generator, an 11-mm strip of tendon was removed from the distal end of a frog sartorius muscle that had exerted a maximum tetanic tension of 270 kdyn. One end was tied as described in the Methods section to the displacement generator and a similar tie was made at the other end to the force transducer, leaving 7.5 mm of free tendon between the ties. The passive length-force curve of the tendon obtained during a quick release lasting 150–300  $\mu$ s was exponential, being fitted by the curve,  $P = 244 \exp(-\Delta l / 16.4)$ , where  $P$  is in kdyn and  $\Delta l$  is the release in micrometers. An accurate length-force curve could be obtained in this manner because the transmission time along the tendon was small (see Discussion). The transmission time was less than 22  $\mu$ s at  $P \approx 4$  kdyn and less than 8  $\mu$ s for  $P > 190$  kdyn. When the tendon was retied so that 1.5 mm of tendon remained free, the transmission time was approximately 5  $\mu$ s for all tensions greater than 100 kdyn. This implies that in our muscle preparations the extra lag associated with the tie per se was less than 2  $\mu$ s. The propagation time along the tendon at tensions greater than 0.6  $P_o$  was less than 0.5  $\mu$ s/mm [(8–5)/(7.5–1.5)].

#### *Calculation of Stiffness*

The formulae in the Introduction were derived under the simplifying assumption of zero internal viscosity. In this case, for semitendinosus bundles the calculated stiffness,  $\xi_{-1}$  (Eq. 8), was  $266 \pm 44$  ( $N = 7$ ).

In whole sartorius muscle the calculation is slightly more complex because of the dispersion of fiber length. In the sartorius of *Rana pipiens pipiens* the length of the shortest muscle fibers,  $L_s$ , is 0.6–0.7 times the length of the

longest fibers,  $L$  (unpublished observations). Assuming  $L_{\text{AVE}} \approx (L + L_s)/2$ , the calculated stiffness,  $\xi_{v-1}$  (Eq. 10), is 200–270, a value similar to that obtained for semitendinosus bundles. As shown later, this calculated stiffness of about 240 (corresponding to a compliance of 45 Å per half sarcomere) places an upper limit on striated muscle stiffness.

The value of  $\xi_{v-1}$  for the five *Rana pipiens berlandiari*, calculated from Eq. 10 using  $L_s = 0.6 L$  and  $L_{\text{AVE}} = 0.8 L$  was significantly larger than the corresponding value for *Rana pipiens pipiens*. This may have been due to differences in muscle geometry (perhaps  $L_s$  was not equal to 0.6–0.7  $L$  in this subspecies) but this possibility was not explored at the time the measurements were made. Consistent with this possibility is the fact that conduction velocity in the *berlandiari sartorii*, calculated as  $0.6 L/\tau$ , was also significantly different from that calculated for the *pipiens sartorii* ( $220 \pm 7$  mm/ms,  $N = 5$  versus  $175 \pm 4$ ,  $N = 13$ ), whereas the value calculated for *pipiens* semitendinosus bundles ( $L/\tau = 169 \pm 11$ ,  $N = 7$ ) was not significantly different.

#### DISCUSSION

At present there is no clearly satisfactory way of measuring the absolute value of the instantaneous compliance of muscle. Measurement of the force-displacement curve during a quick release (6) presents two difficulties. If the release is done too slowly, the force displacement relationship is distorted by cross-bridge turnover and/or time-dependent relaxation of existing cross bridges. If it is done too quickly, the finite transmission time down the muscle means sarcomeres near the released end are initially overshorted and those distant remain initially unchanged. It requires several transmission times for the disturbance (quick release) to be distributed uniformly along the muscle; measurements recorded before this occurs are distorted by the longitudinal nonuniformity. If one simply records the force at the end of a quick displacement (3) one has the same difficulties, quick releases in this case resulting in an overshoot in the recorded force drop, due to the initial overshorting of the proximal sarcomeres. The quicker the release, relative to the transmission time, the larger the overshoot. The direct measurement of transmission time avoids both of these difficulties, although other problems arise, as discussed later.

The use of transmission time to measure the stiffness of muscle appears to have been first suggested in an abstract by Truong et al. (9). More recently, Blangé et al. (10, 11) have made use of a similar phenomenon, namely the oscillations that follow the extremely quick release of a muscle. In the rat soleus this phenomenon, which is related to the initial longitudinal nonuniformity, can persist for several milliseconds, whereas in frog sartorius, it is damped out fairly rapidly (10). For a simple elastic rod both the transmission

time and the oscillatory frequency provide identical information. For a muscle they do not, because a muscle is likely nonlinear and also time variant.

#### *Measurement Time*

An advantage of the transmission time measurement is that it is related to the instantaneous stiffness at the moment of release, since it detects perturbations that are only the order of 0.1%  $P_o$ . Even though the transmission time for longer muscles might be as long as 0.2 ms, with this technique one measures the propagation of the *front* of the disturbance along regions of the muscle which have not yet been affected in any way by the release. The measurement is, therefore, essentially instantaneous, limited only by the acceleration of the speaker coil. As a result, it is practically undisturbed by cross-bridge turnover or changes in orientation which might occur during measurements that take longer to complete (3, 10, 11). The measurement of oscillation frequency, on the other hand, is related to the stiffness after release and takes at least one cycle to complete.

The measurement of transmission time, of course, cannot be absolutely instantaneous, since the force must drop a finite amount before the drop is detectable. The solution of the equation for longitudinal propagation of impulses along an undamped spring (Appendix) together with Eq. 6 shows that the initial drop in force at the distal end is  $\Delta P/P_o = 2 \xi (v/c)$  where  $v$  is the initial velocity of release at the proximal end and  $c$  is the propagation speed. It was found that the initial speaker displacement,  $U$ , could be described by the equation  $U = \alpha t^3$  where  $\alpha = 5 \times 10^8$  cm/s<sup>3</sup>. Substituting  $v = 3\alpha t'^2$  one may then solve for  $t'$ , the measurement time. Taking as worst case values,  $\Delta P/P_o = 5 \times 10^{-3}$ ,  $\xi = 100$ ,  $c = 10^4$  cm/s, yields a measurement time of about 15  $\mu$ s.

#### *Effect of Tendons*

Another advantage of the transmission time technique is that it minimizes the effect of the tendon connections on the measurement of stiffness. The tibial tendon of the frog sartorius muscle bifurcates into two tapered portions, with fibers inserting along the tapered portion through very short tendons. At the pelvic end, fibers insert through fine tendons onto a tendonous sheet which attaches to the pelvis. The very short tendons, the fine tendons, and the pelvic sheet do not contribute any significant delay in the transmission time measurement. This is seen by substituting  $\xi = KL/P_o$  from Eq. 6 into Eq. 8 and solving for  $\tau$ , yielding

$$\tau = \left( \frac{Mv}{K} \right)^{1/2}. \quad (11)$$

The compliance of any of these components of the tendon system can at most be equal to that of active muscle (12). Their mass is substantially less than the mass of muscle fibers and  $\nu$  for muscles is not too different from unity (see Discussion) so that from Eq. 11 even if the  $K$  for any of the nonmassive tendon components was the same as that of muscle, the transmission time along it would be much less.

In the whole sartorius muscle, fibers insert onto the tapered region of tendon all along its length so, as a reasonable first approximation, one might assume that the cross-sectional area of the tendon at any point is proportional to the number of fibers that have inserted onto the tendon proximal to that point, and is, therefore, proportional to the tension it bears at that point. For this case it can be shown for an exponential compliance that the total transmission time along a tapered tendon having a maximum cross-sectional area of  $A_0$  is the same as for an equal length of untapered tendon of area  $A_0$  having the entire force,  $P_0$ , inserting at its end. The transmission time along the untapered region of tendon of the frog sartorius for forces near  $P_0$  is less than  $0.5 \mu\text{s}/\text{mm}$  (see Results). In a whole 30-mm sartorius muscle the tapered region of tendon from the shortest fibers to the tie can be as long as 12 mm, so in the whole muscle the measured transmission time may be some  $8 \mu\text{s}$  greater than the transmission time along the shortest fibers (including the delay of the tie). In the muscle bundles, the amount of tendon is greatly reduced so that the total extra delay is likely no more than  $4 \mu\text{s}$ . Since these corrections are relatively small they were not applied to the data in Tables I and II.

#### *Relation between Transmission Time and Muscle Compliance*

It was important to ascertain that the transmission times we measured were primarily related to the compliance of the cross bridges rather than something parallel. The evidence for this is twofold. One is the observation that transmission time changes with activation and the other is the extreme sensitivity of the transmission time in iodoacetate-poisoned muscle to stretches and releases the order of 3% of muscle length. The only structures known to be affected this way by activation or iodoacetate are the cross bridges. It was not possible to determine whether the measured compliance resided entirely in the cross bridges or whether part of it resided in series with the cross bridges. Huxley and Simmons (5) suggest from the results of their experiments on stretched muscles (Fig. 14) that all of the series compliance resides in the cross bridges. However, their results do not rule out the possibility of an exponential compliance in series with the cross bridges. Our experiments also do not distinguish between these two possibilities.

A difficulty in ascertaining the precise stiffness is the presence of internal viscosity within the muscle. This would tend to shorten the transmission



time, making the muscle appear stiffer than it actually is. Because of this, the actual compliance of muscle may be greater than the value calculated for the simple elastic model with  $\nu = 1$ , the latter being the lower limit for compliance.

Another difficulty in obtaining the exact stiffness is the possibility that not all of the muscle mass participates in the propagation of small disturbances. For example, it is possible that the extracellular water and the sarcoplasmic reticulum, which comprise approximately 30% of the muscle mass, do not participate in the propagation of the disturbance. In this case we would have  $\nu = 0.7$  and  $\xi = 140$ –190. This corresponds to a compliance of 55–80 Å per half sarcomere, not too different from the compliance of 85 Å per half sarcomere obtained by Huxley and Simmons (3). If the values of Huxley and Simmons for the compliance near  $P_0$  are correct, and it is valid to exclude the sarcoplasmic reticulum and extracellular water from the dynamic mass, then virtually the entire myofibrillar space (the myofibrils plus most of the associated water) participates in the propagation of rapid disturbances. Clearly more than just the myofilaments, which comprise in mass only 15–25% of the muscle, must participate dynamically since to assume otherwise gives  $\nu = 0.15$ –0.25, an assumption which leads to an unrealistically large compliance.

The problem in simply assuming  $\nu = 1$  is dramatically demonstrated in our experiments on partially activated whole muscles (Table III). For a 50% decrease in  $P_0$  (implying approximately half the fibers activated),  $\xi_{-1}$  increased 1.7-fold. The apparent increase in stiffness with decreasing activation is clearly due not to any real increase in the stiffness of a single fiber, but to the faulty assumption  $\nu = 1$  while an increasing fraction of the total muscle mass no longer participates in the transmission of the signal.

The effect of partial activation upon transmission time is also interesting. From Eq. 8, if  $\nu$  scales directly with  $P_0$  during partial activation, the transmission time would be independent of activation since the nondimensional stiffness for each fully activated fiber,  $\xi$ , should remain constant. To a first approximation this is true, a 50% decrease in force resulting in only a 9% increase in  $\tau$ . However, as more fibers become inactive, there is a greater increase in  $\tau$ . This suggests that when only a small number of the fibers are active, some of the inactive fibers, which are connected to the active ones through the perimysium and endomysium, are dragged along during a rapid displacement, leading to a smaller decrease in  $\nu$  than in  $P_0$ .

#### *Possible Application of the Transmission Time Measurement*

If the values of  $\nu$  and viscosity are not affected by shortening velocity, the present methodology can be used to measure the relative stiffness of a given preparation in various physiological states. Thus it should be possible to find

out whether a muscle when shortening is more or less stiff than when it is contracting isometrically. This result would be of interest because it gives information about the relative number of cross bridges in the two states, which is an important point of distinction in different models of the contractile mechanism (4, 5).

#### APPENDIX

In this appendix, equations for a simple model, adequate to explain some of the short time-scale phenomena of muscle, are derived. These are solved to obtain an analytic expression for the short-time relation between force and displacement in the absence of viscosity.

Consider an elastic rod of length  $L$  and density  $\rho$ . Let  $x$  represent distance along the elastic rod and  $u$  the local displacement. The end  $x = 0$  is driven with a displacement  $u(0, t) = U(t)$  where  $U(t) \equiv 0$  for  $t < 0$  and the end  $x = L$  is attached to a rigid force transducer. Looking at two locations along the rod separated by a distance  $dx$ , we have the following diagram (Fig. 5).

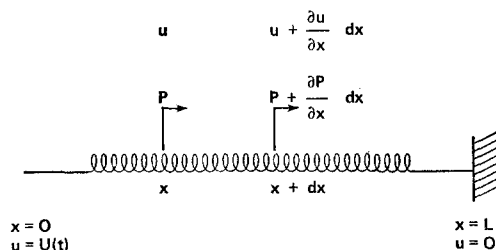


FIGURE 5

For such an elastic body, ignoring viscous forces, we may write the equivalent of Hooke's law

$$P/A = -E \frac{\partial u}{\partial x}, \quad (1a)$$

where  $P$  is force and  $A$  is the area upon which Young's modulus,  $E$ , is based (see Eq. 4 of text). Considering the element of rod between  $x$  and  $x + dx$  we may write the force equation,

$$P - (P + \frac{\partial P}{\partial x} dx) = (\rho A dx) \frac{\partial^2 u}{\partial t^2},$$

so that

$$-\frac{\partial P}{\partial x} = \rho A \frac{\partial^2 u}{\partial t^2}. \quad (2a)$$

Taking the partial derivative of Eq. 1 a with respect to  $x$ , substituting into Eq.

2 *a* for  $\partial P/\partial x$  and canceling *A* in each term yields

$$E \frac{\partial^2 u}{\partial x^2} = \rho \frac{\partial^2 u}{\partial t^2}. \quad (3 a)$$

Eq. 3 *a* is the simple wave equation. The solution to Eq. 3 *a* which satisfies the boundary conditions of the present problem is

$$u(x, t) = \sum_{n=0}^{\infty} [U(t - x/c - 2nL/c) - U(t + x/c - 2nL/c - 2L/c)], \quad (4 a)$$

where  $c = (E/\rho)^{1/2}$ . Eq. 4 *a* shows that the solution may be thought of as the sum of right-running and reflected left-running waves along the rod.

The force may be found by applying Eq. 1 *a* to Eq. 4 *a* which gives

$$P(x, t) = (EA/c) \left[ \sum_{n=0}^{\infty} \{U'(t - x/c - 2nL/c) + U'(t + x/c - 2nL/c - 2L/c)\} \right], \quad (5 a)$$

where  $U'$  denotes differentiation of  $U(t)$  with respect to  $t$ .

At  $x = L$  we have

$$P(L, t) = 2(EA/c) \left[ \sum_{n=0}^{\infty} U'(t - L/c - 2nL/c) \right]. \quad (6 a)$$

For short times, the relation between force at the distal end and displacement at the proximal end is simply

$$P(L, t) = 2[EA/c] U'(t - L/c). \quad (7 a)$$

The equipment used in these experiments was originally designed by Mel N. Kronig, Biomedical Engineering and Instrumentation Branch, Division of Research Services, National Institutes of Health. Walter Friauf provided valuable advice concerning modification of this design.

We are grateful to Drs. Tugendhold Blangé and August E. J. L. Kramer and to Professor Andrew F. Huxley for helpful discussions concerning the influence of internal viscosity on transmission time.

*Note Added in Proof* Since submission of this manuscript, X. T. Truong has published a paper in which the propagation speed in activated frog sartorius muscle is measured by determining the phase angle shift between the local displacement at two points along the muscle while driving one end of the muscle sinusoidally. At a frequency of 3 kHz, he found the apparent phase velocity to be approximately 130 m/s for active muscle compared with 60 m/s for the passive muscle. (Truong, X. T. 1974. *Am. J. Physiol.* **226**:256-264.)

Received for publication 14 December 1973.

#### REFERENCES

1. HUXLEY, A. F. 1957. Muscle structure and theories of contraction. *Prog. Biophys. Biophys. Chem.* **7**:255-318.

2. PODOLSKY, R. J., A. C. NOLAN, and S. A. ZAVELER. 1969. Cross-bridge properties derived from muscle isotonic velocity transients. *Proc. Nat. Acad. Sci. U. S. A.* 64:504-511.
3. HUXLEY, A. F., and R. M. SIMMONS. 1971. Proposed mechanism of force generation in striated muscle. *Nature (Lond.)*. 233:533-538.
4. PODOLSKY, R. J., and A. C. NOLAN. 1972. Muscle contraction transients, cross-bridge kinetics, and the Fenn effect. *Cold Spring Harbor Symp. Quant. Biol.* 37:661-668.
5. HUXLEY, A. F., and R. M. SIMMONS. 1972. Mechanical transients and the origin of muscular force. *Cold Spring Harbor Symp. Quant. Biol.* 37:669-680.
6. HILL, A. V. 1950. The series elastic component of muscle. *Proc. R. Soc. Lond. B Biol. Sci.* 137:273-280.
7. HILL, A. V. 1970. *In Experiments in Muscle Mechanics*. Cambridge University Press, London. 79-81.
8. SANDOW, A. 1947. Latency relaxation and a theory of muscular mechano-chemical coupling. *Ann. N. Y. Acad. Sci.* 47:895-929.
9. TRUONG, X. T., S. M. WALKER, and B. J. WALL. 1963. The use of velocity of elastic waves in the determination of elastic constants in frog muscle. *Physiologist*. 6:289.
10. BLANGÉ, T., J. M. KAREMAKER, and A. E. J. L. KRAMER. 1972. Tension transients after quick release in rat and frog skeletal muscles. *Nature (Lond.)*. 237:281-282.
11. BLANGÉ, T., J. M. KAREMAKER, and A. E. J. L. KRAMER. 1972. Elasticity as an expression of cross-bridge activity in rat muscle. *Pfluegers Arch. Eur. J. Physiol.* 336:277-288.
12. JEWELL, B. R., and D. R. WILKIE. 1958. An analysis of the mechanical component in frog's striated muscle. *J. Physiol. (Lond.)*. 143:515-540.